Dual-band frequency selective surface with large band separation and stable performance*

Zhou Hang(周 航)[a], Qu Shao-Bo(屈绍波)[a]†, Peng Wei-Dong(彭卫东)[b],
Lin Bao-Qin(林宝勤)[a], Wang Jia-Fu(王甲富)[a], Ma Hua(马 华)[a],
Zhang Jie-Qiu(张介秋)[a], Bai Peng(柏 鹏)[b], Wang Xu-Hua(王徐华)[b], and Xu Zhuo(徐 卓)[c]

[a] *College of Science, Air Force Engineering University, Xi'an* 710051, *China*

[b] *Synthetic Electronic Information System Research Department, Air Force Engineering University, Xi'an* 710051, *China*

[c] *Electronic Materials Research Laboratory, Key Laboratory of the Ministry of Education, Xi'an Jiaotong University, Xi'an* 710049, *China*

(Received 12 October 2011; revised manuscript received 2 November 2011)

A new technique of designing a dual-band frequency selective surface with large band separation is presented. This technique is based on a delicately designed topology of L- and Ku-band microwave filters. The two band-pass responses are generated by a capacitively-loaded square-loop frequency selective surface and an aperture-coupled frequency selective surface, respectively. A Faraday cage is located between the two frequency selective surface structures to eliminate undesired couplings. Based on this technique, a dual-band frequency selective surface with large band separation is designed, which possesses large band separation, high selectivity, and stable performance under various incident angles and different polarizations.

Keywords: dual-band frequency selective surface, Faraday cage

PACS: 41.20.–q, 73.20.–r **DOI:** 10.1088/1674-1056/21/5/054101

1. Introduction

A frequency selective surface (FSS) is a periodic assembly of one- or two-dimensional resonant structures that exhibits band-pass or band-stop responses. For more than four decades, FSSs have attracted much attention because of their comprehensive applications, such as polarizers, fliters, subreflectors, and band-pass hybrid radomes.[1−6] In some applications, multiband FSSs are needed for the design of dual-reflector antennas. The use of a multiband FSS makes it possible to share a main reflector in different frequency bands. In addition, multiband FSSs have proven to be an efficient way of increasing satellite communication capabilities. In such applications, FSSs with multiple independent transmission bands are required. Early research mainly focused on multi-concentric elements, such as ring and square loops, to construct the multiband FSSs.[7,8] Two FSSs cascaded on complementary surface layers were proposed in Refs. [9] and [10]. Fractal elements were discussed to design the multiband FSS in Ref. [11]. Miniaturized dual-band FSSs with close band separation by using lumped elements were presented in Ref. [12].

In some applications, especially in military systems, dual-band FSSs with large band separation are much more attractive because they can avoid the interference and reduce the risk of radar detection. However, the band separation of a dual-band FSS is generally not very large, since the dimensions of a conventional FSS are about half the resonant wavelength, resulting in grating lobes that can badly disturb the performance of the higher frequency pass-band. Furthermore, the conventional FSS is sensitive to different incident angles and different polarizations. Such problems would be more evident especially when the lower pass-band lies in a low frequency range.

Under the aforementioned considerations, we present a new technique of designing dual-band FSSs with large band separation. The technique is based on properly designed topologies of L- and Ku-band

*Project supported by the National Natural Science Foundation of China (Grant Nos. 60871027, 60901029 and 61071058), the National Basic Research Program of China (Grant No. 2009CB623306), the Research Fund of Shaanxi Key Laboratory of Electronic Information System Integration, China (Grant No. 201114Y11), the Postdoctoral Science Foundation of China (Grant No. 20100481327), and the Natural Science Foundation of Shaanxi Province, China (Grant No. 2011JQ8031).

†Corresponding author. E-mail: Qushaobo@mail.xjtu.edu.cn

© 2012 Chinese Physical Society and IOP Publishing Ltd

filters. The capacitively-loaded square loop structure is selected to generate the L-band pass-band, because its size can be made much smaller than the operating wavelength by changing the capacitor. Such a small structure will effectively restrain the grating lobes at lower frequencies. The aperture-coupled FSS was firstly proposed in Ref. [13], and further studied in Refs. [14] and [15], in which two patches were coupled through an aperture to form a higher-order band-pass filter. Such an FSS possesses higher selectivity and a flat pass-band. Because of this, we select the aperture-coupled FSS to generate the Ku-band pass-band. Then the two band-pass structures are synthesized to form a dual-band FSS. A Faraday cage is installed between the two structures to eliminate undesired couplings. Using this technique, a dual-band FSS with large band separation is designed. The design procedure and the results of the FSS are presented and discussed as follows.

2. Design process and results

Figure 1 shows the geometry of the proposed FSS structure. Each unit cell consists of a capacitively-loaded square loop surrounded by a Faraday cage and a three-layered aperture-coupled FSS. A three-dimensional (3D) view of the unit cell is shown in Fig. 1(d). As can be seen, it is composed of three metallic layers separated by two thin dielectric layers. On the surface of the unit cell, four chip capacitors are loaded between the square metallic patch and the square metallic loop. And four L-shape metallic patches are arranged around the square metallic loop on the four corners. The middle metallic layer is etched with L-shape apertures of the same topology on the four corners. A Faraday cage, which is composed of 28 metallic stubs, is arranged between the top and the middle metallic layers. The bottom metallic layer is etched with only four L-shape patches of the same topology on the four corners as that in the top layer. For this particular topology, when the unit cell is expanded periodically in the x- and the y-axis directions, an infinite size FSS composed of a capacitively-loaded filter and an aperture-coupled filter is obtained.

Geometrical dimensions of the structure are $p_1 = 10.8$ mm, $p_2 = 8.0$ mm, $a = 4.4$ mm, $l_\mathrm{p} = 9.0$ mm, $w_\mathrm{p} = 2.0$ mm, $s = 6.0$ mm, $l_\mathrm{s} = 1.8$ mm, and $w_\mathrm{s} = 0.6$ mm. The capacitance of the chip capacitor is $C_1 = 3.0$ pF. In order to form an effective Faraday cage, the conditions of $d/\gamma_0 \leq 0.1$ and $d/d_\mathrm{p} \geq 0.5$ must be satisfied,[16] where d and d_p are the diameter and the periodicity of the metallic stub, respectively. We chose $d = 0.6$ mm and $d_\mathrm{p} = 1.0$ mm. The 28 metallic stubs are arranged to form a Faraday cage. The FSS arrays have a two-layered substrate ($\varepsilon_\mathrm{r} = 2.65$, $\tan\delta = 0.001$) with a thickness of 0.6 mm.

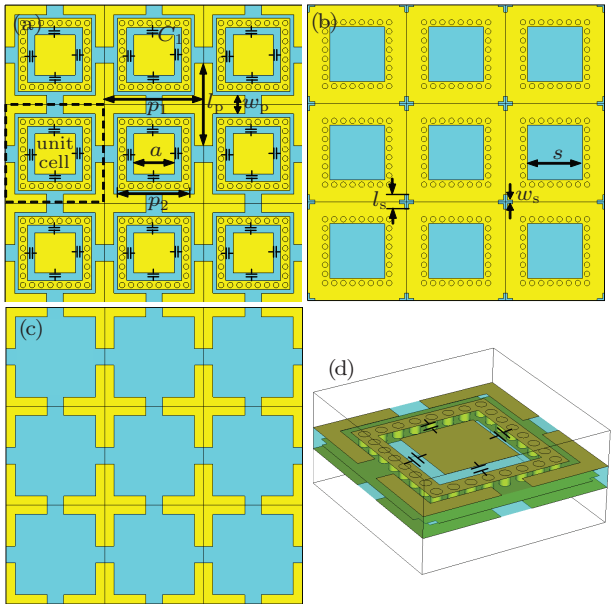


Fig. 1. (colour online) Geometric configuration of the FSS structure: (a) top view, (b) back view of the middle layer, (c) back view, and (d) 3D view of a unit cell.

We use CST Microwave Studio to calculate its reflection and transmission characteristics. We assume that the FSS is an infinite periodic structure. The FSS is excited by an incident plane wave, which is set at different incident angles and with different polarizations. The four sides of the unit cell are set to meet the periodic boundary conditions. Figure 2 gives the transmission spectra under normal incidence. As observed, there are two evident band-pass responses. The −3 dB bandwidths of the lower and the upper pass-bands are 30 MHz (1.95–1.98 GHz)

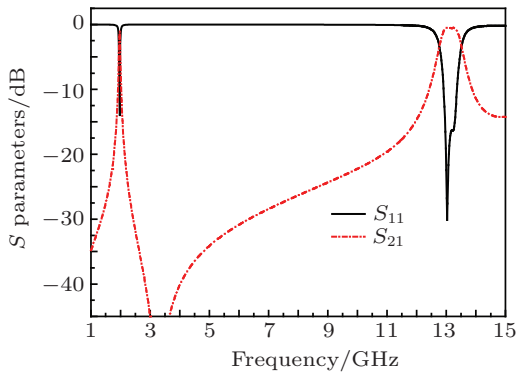


Fig. 2. (colour online) The S parameter of the structure.

and 710 MHz (12.80–13.51 GHz), respectively. The insertion losses of the two pass-bands are 1.2 dB and 0.51 dB, respectively. In order to clarify the physical mechanism of the FSS, we will analyze to the two resonances in the following section.

3. Analysis

3.1. L-band passband

The L-band response is illustrated in Fig. 3. Figure 3(a) shows the surface current distribution for the incident wave at 1.97 GHz with transverse-electric (TE) polarization. As observed, there are two symmetrical current loops on the surface, and there is no current flowing through the transverse capacitors. Based on this current distribution, the corresponding equivalent circuit model is given in Fig. 3(b).

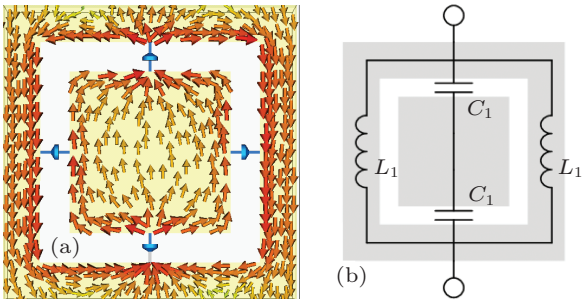


Fig. 3. (colour online) (a) Surface current distribution at 1.97 GHz and (b) the equivalent circuit model.

The inductance L_1 can be approximately calculated from the following formula:[17]

$$L_1 = 2\times10^{-4}l\left[\ln\frac{l}{w+t}+1.93+0.2235\left(\frac{w+t}{l}\right)\right]K_{\rm g},$$

where $K_{\rm g} = 0.57 - 0.145\ln\frac{w}{h}$, $\frac{w}{h} > 0.05$, L, w, and t are the length, the width, and the height of the metallic line, respectively. Units for the dimensions in the formula are micrometer. Here, $w = 1000$ μm, $h = 1200$ μm, $l = 16000$ μm, and $t = 17$ μm, so $L_1 = 8.9703$ nH. The circuit in Fig. 3(b) can be seen as a circuit in which two parallel inductances are connected in parallel with two series capacitances. So the resonant frequency is

$$f_0 \approx \frac{1}{2\pi\sqrt{\frac{1}{2}L_1\times\frac{1}{2}C_1}} = 1.94\ (\text{GHz}),$$

which is close to the simulation result of 1.97 GHz.

For the transverse-magnetic (TM) polarization, the model will be the same except that the operating capacitances become transverse.

3.2. Ku-band passband

For the Ku-band band-pass response of the aperture-coupled FSS, the electric field distributions at 13.06 GHz in the passband are shown in Fig. 4. For the TE polarization, the surface electric field distribution is shown in Fig. 4(a). It can be found in Fig. 4(a) that the electric resonance occurs in the crossed metallic patches on the two sides of the FSS. The Faraday cage formed by the metallic stubs effectively prevents the electromagnetic wave from entering into the middle region of the FSS. Thus, the coupling between L- and Ku-band microwave filters will be effectively eliminated. Accordingly, the Ku passband arises from the enhanced transmission assisted by the coupling aperture. For the TM polarization, the situation will be the same except that the resonant electric fields on the patches become transverse, as shown in Fig. 4(b).

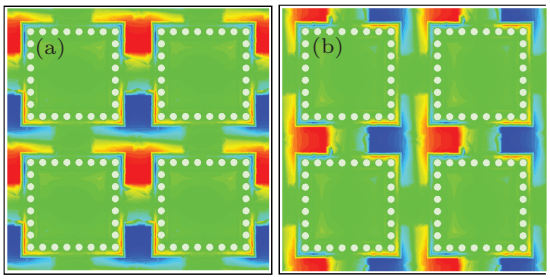


Fig. 4. (colour online) Electric field distribution diagrams at 13.06 GHz for (a) the TE and (b) the TM polarizations.

3.3. FSS with stable performance

As is well known, in the practical applications, it is necessary that the FSS provides stable performance under different incidence angles and different polarizations. Figure 5 gives the frequency responses for different incidence angles and different polarizations. From Fig. 5, we can find that the two passbands are stable for incident angles within 30° of the normal direction and different polarizations.

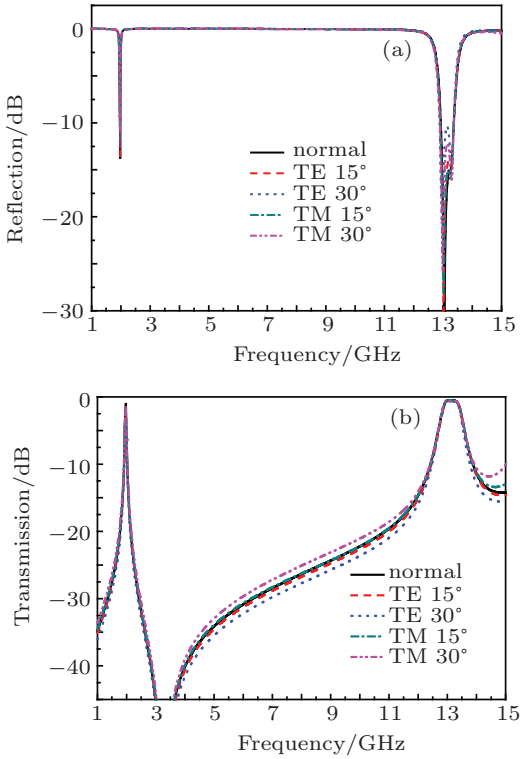


Fig. 5. (colour online) Frequency responses of (a) reflection and (b) transmission under different polarizations and various incident angles.

4. Discussion

A new technique of designing the dual-band FSS is proposed. Based on this technique, a dual-band FSS with large band separation is designed, which possesses large band separation, high selectivity, and stable performance for incident angles within 30° of the normal direction and different polarizations. Nevertheless, it still requires further improvement. The lumped elements and the multi-layered FSS are used to generate L and Ku passbands, respectively. Such a configuration is comparatively complex, expensive, and not very easy to fabricate. On the other hand, the dimensions of the aperture-coupled structure for the Ku band is comparable to the operating wavelength, so it will be more sensitive at a large incident angle. To improve the performance of the FSS, some other miniature elements or thicker substrates may be studied.

5. Conclusion

In this paper, we propose a technique of designing dual-band FSSs with large band separation. This technique is illustrated and demonstrated by a specific design of a dual-band FSS through the field analysis and the full wave simulation. The dual-band FSS has advantages of high selectivity, large band separation, stable performance, and compact size. Such an FSS can provide practical applications in communications, electronic countermeasures, etc.

References

[1] Munk B A 2000 *Frequency Selective Surfaces: Theory and Design* (New York: Wiley)

[2] Wu T K 1995 *Frequency Selective Surface and Grid Array* (New York: Wiley)

[3] Jia H Y, Gao J S, Feng X G and Sun L C 2009 *Acta Phys. Sin.* **58** 505 (in Chinese)

[4] Jun L, Sun G C and Wang J B 2009 *Chin. Phys.* B **18** 1598

[5] Meng Z J, Wang L F, Lv M Y and Wu Z 2010 *Chin. Phys.* B **19** 127301

[6] Wang J B and Lu J 2011 *Acta Phys. Sin.* **60** 057304 (in Chinese)

[7] Wu T K 1994 *IEEE Trans. Antennas Propag.* **42** 1659

[8] Huang J, Wu T K and Lee S W 1994 *IEEE Trans. Antennas Propag.* **42** 166

[9] Lockyers D S, Vardaxpglou J C and Simpkin R A 2000 *IEE Pro. Micro. Antennas Propag.* **147** 501

[10] Hu X D, Zhou X L, Wu L S, Zhou L and Yin W Y 2009 *IEEE Antennas Wireless Propag. Lett.* **8** 1374

[11] Romeu J and Rahamat-Samii Y 2000 *IEEE Trans. Antennas Propag.* **48** 1097

[12] Xu R R, Zhao H C, Zong Z Y and Wu W 2008 *IEEE Microw. Wireless Compon. Lett.* **18** 782

[13] Pous R and Pozar D M 1991 *IEEE Trans. Antennas Propag.* **39** 1763

[14] Tamijani A, Sarabandi K and Rebeiz G M 2004 *IEEE Trans. Microwave Theory Tech.* **52** 1781

[15] Behdad N, Joumayly M and Salehi M 2009 *IEEE Trans. Antennas Propag.* **57** 460

[16] Zhang Y L, Hong W, Wu K, Chen J X and Tang H J 2005 *IEEE Trans. Microw. Theory Tech.* **53** 1280

[17] Inder B and Prakash B 2003 *Microwave Solid State Circuit Design* (New York: Wiley)